Ordered Ni nanohole arrays with engineered geometrical aspects and magnetic anisotropy

D. Navas,[a] M. Hernández-Vélez,[b] and M. Vázquez
Instituto de Ciencia de Materiales, CSIC, 28049 Cantoblanco (Madrid), Spain

W. Lee and K. Nielsch
Max-Planck-Institut für Mikrostrukturphysik, 06120 Halle, Germany

(Received 8 February 2007; accepted 13 April 2007; published online 7 May 2007)

Ni nanohole arrays are prepared by a replication process involving sputtering, polymer molding pressing, and electroplating techniques, using anodic alumina membranes as templates. Nanohole diameter to interhole distance ratio is engineered by suitable template processing. From the analysis of the magnetization curves for increasing nanohole diameter, it is concluded that coercivity increases due to the pinning of domain walls to nanoholes, while in-plane anisotropy decreases owing to local shape anisotropy effects. © *2007 American Institute of Physics*.
[DOI: 10.1063/1.2737373]

Highly ordered nanostructures consisting of nanopore and nanohole arrays are recently attracting great attention due to their application in high density magnetic storage media.[1] Different magnetic hole arrays are prepared by lithographic patterning[1,2] and by alternative less expensive techniques.[3] For example, nanoporous membranes have been used as templates.[4] The geometry of nanoporous membrane can be identically transferred to different films by successive replica/antireplica processes. Various routes have been proposed where the final replicated nanostructures consist of highly ordered nanohole or nanochannel arrays (e.g., in glass or polymeric membranes).[5] Recently, metal nanohole arrays based on the replication of anodic alumina membrane (AAM) have been reported.[6] In nanohole magnetic films, the holes act themselves as pinning centers for the wall displacements and their periodic distribution determines the whole magnetization process.[1,2]

The objectives of the present report have been (i) the design and fabrication of ordered Ni nanohole arrays, (ii) the tailoring of nanohole diameter while keeping constant the interhole distance, and (iii) the magnetic characterization of the magnetization process analyzing the coercivity and magnetic anisotropy.

Two-step anodized AAM has been used as initial templates. A scheme of preparation processes is presented in Fig. 1. Nanoporous anodic alumina membranes were grown from high-purity (99.999%) Al foils by two-step anodization process, as described elsewhere.[6,7] Main features of AAM templates [Fig. 1(a)] are pore diameter (d) of around 35 nm, interpore distance (D) of 105 nm, and pores self-assembling into close packed structure in 2×2 μm^2 size domains. To gradually increase the hole diameter, a controlled widening process was performed by immersing the AAMs in 5 wt. % phosphoric acid solution at 35 °C for a range of time intervals, with a dissolution speed of 0.75 nm/min. Thus, the final pore diameters of nanoholes ranged from 35 to 70 nm. Afterwards, a 15 nm thick Au layer was sputtered onto the surface of the AAM, serving as an active electrode for subsequent electroplating [Fig. 1(b)]. Then, melted poly(methyl methacrylate) (PMMA) was pressed into the AAM to fill in the holes [Fig. 1(c)]. Two selective chemical etchings were used to remove both the Al substrate (a solution of 50 ml HCl, 3.4 g $CuSO_4$, and 100 ml H_2O) and the alumina membrane (dipping the sample into a 30 wt. % phosphoric acid solution). Hexagonally ordered arrays of PMMA nanopillars were thus obtained with a Au thin film at the bottom [Fig. 1(d)]. Subsequently, Ni was electroplated using the Au layer as cathode [Fig. 1(e)] and Watts-Bath (300 g/l $NiSO_4\cdot6H_2O$, 45 g/l $NiCl_2\cdot6H_2O$, and 45 g/l H_3BO_3, pH =4.5) as electrolyte. Electroplating was performed at 35 °C for 10 min with 1 mA/cm^2 current density and magnetic stirring. Finally, the PMMA nanostructure was removed by chemical action of chloroform, and a freestanding Ni membrane was obtained [Fig. 1(f)]. Typical thickness of Ni membranes was around 200 nm. To complete the study, a continuous Ni thin film was prepared under the same electroplating conditions.

Morphological characterization was carried out with a Jeol High Resolution Scanning Electron Microscopy (HRSEM) model JM6400. Figure 2 shows the HRSEM images of the Au surfaces of Ni membranes with different hole diameters. The morphological features of the AAMs templates are exactly replicated at the Au surface. However, some differences are observed in the Ni surfaces HRSEM

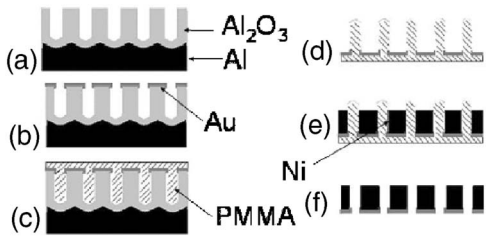

FIG. 1. Preparation of Ni nanohole arrays from porous alumina membrane (a): a Au nanolayer is sputtered onto the top of the membrane (b); PMMA polymer is pressed to fill in the pores (c); after flipping, a polymeric pillar array on a solid polymeric layer remains after Al and Al_2O_3 are removed (d); Ni is electroplated using the Au layer electrode (e); Ni nanohole array is obtained after removing the polymer (f).

[a]Author to whom correspondence should be addressed; electronic mail: danavas@icmm.csic.es
[b]Permanent address: Applied Physics Department, C-XII, UAM, Cantoblanco 28049, Madrid, Spain.

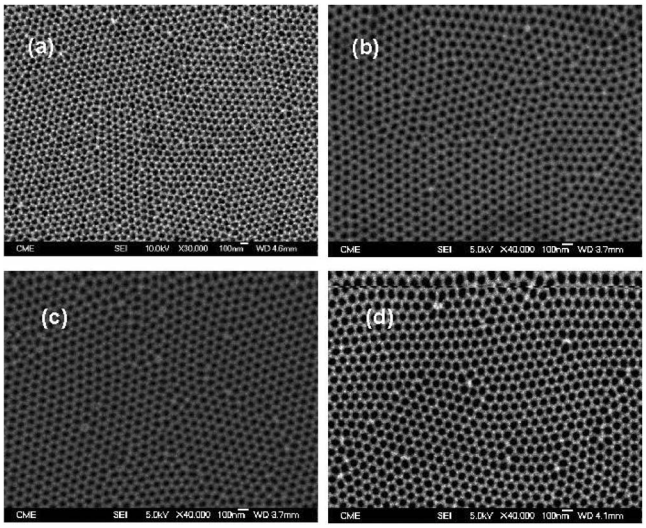

FIG. 2. HRSEM images of Ni nanohole arrays replicating the template hole diameters of 35 nm (a), 50 nm (b), 62 nm (c), and 70 nm (d).

images. The ordering of the AAM is only perfectly replicated into the metallic membranes with higher diameters (d=62 and 70 nm). To understand it, we should consider that for AAM templates with the smallest pore diameters (d =35 nm), the process of filling the pores with PMMA [Fig. 1(c)] becomes harder and, subsequently, the height of the polymeric pillars [Fig. 1(d)] is shorter. In this way, during the Ni electroplating, the metal can overflow the polymeric columns, giving rise to the growth of a metallic film covering the PMMA template, and a Ni antidot film is created instead of a nanohole film. For samples with intermediate pore diameter (d=50 nm), only some of the pores in the polymeric template are overflowed with Ni after the electroplating. Therefore, we conclude that a minimum hole diameter of about 60 nm is required to prepare metallic membranes by this technique. To overcome such limitations, a diluted solvent of PMMA and an organic solvent could be alternatively used, which would probably enable an easier filling of the pores even with smaller diameters.

From the technological viewpoint, the proposed fabrication method is proven to be a relative simple and low cost procedure. In Ref. 6 methyl methacrylate monomer was injected into the holes under vacuum and its polymerization was achieved by ultraviolet radiation or by heating (40 °C for 24 h). In the present case, PMMA polymer is melted, pressed [Fig. 1(c)] and after a few minutes the polymeric template is ready for use. Xiao *et al.*[4] reported an alternative way to prepare Ni nanohole arrays with tailored pore diameter and constant interhole distance by sputtering Ni onto AAM templates. It was there observed that for Ni membranes with thickness larger than tens of nanometers, the hole diameter was irregular (gradually decreased from the bottom to the top surface).

Magnetic properties of the continuous Ni film and the different Ni nanohole arrays have been studied by Vibrating Sample Magnetometer (VSM), EG&G Princeton Applied Research, model 155. As an example, Fig. 3 shows the hysteresis loops of Ni nanohole array with 50 nm hole diameter for in-plane and out-of-plane applied field. For in-plane applied field the rather square shaped loop denotes an in-plane magnetization easy axis, while out-of-plane hysteresis loop is typical for hard anisotropy axis (high field to reach magnetic saturation and relatively small coercivity). Previous studies on lithographed nanohole arrays[2–4] were done with in-plane magnetic field applied along different azimuthal orientations in order to determine the magnetization easy axis. It was concluded that the induced easy axes are the directions along which the holes are furthest separated. Here, such measurements are not needed since the holes are well ordered along given orientations but only within domains about 2 $\times 2\ \mu m^2$ average size. Therefore, the effective anisotropy induced by different domains is averaged out for the whole array.

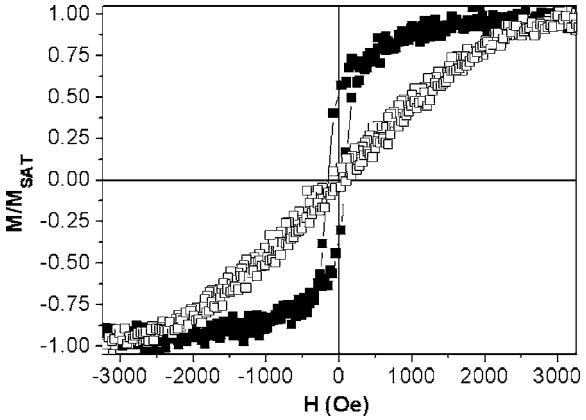

FIG. 3. In-plane (■) and out-of-plane (□) hysteresis loops of Ni nanohole array with 50 nm pore diameter.

Figure 4 shows the in-plane loops for a continuous Ni film and two Ni nanohole arrays with 35 and 62 nm hole diameters. The presence of the holes changes the shape of the loops. While coercivity of the continuous Ni film is 39 Oe, those of Ni hole arrays with 35 and 62 nm hole diameters are 107 and 126 Oe, respectively. That increase of coercivity is ascribed to the pinning of the domain walls to the nanoholes. This variation is consistent with the relationship between coercivity and packing fraction predicted by Hilzinger and Kronmüller.[8]. Coercivity follows a law $H_c \propto 1/(D-d)$, (see inset of Fig. 4), similarly as reported elsewhere.[2] This is explained considering that a stronger pinning effect is expected for decreasing interhole distance ($D-d$). Hence, stronger magnetic field is needed to overcome the pinning and created by the nanoholes. The possibility is

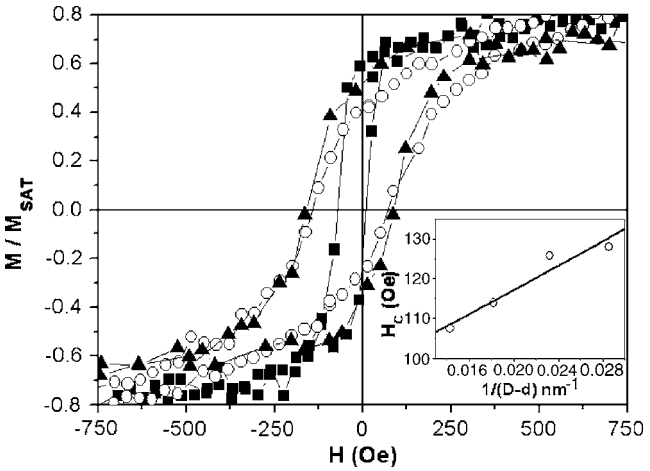

FIG. 4. In-plane loops for continuous film (■) and for two Ni nanoholes arrays [d=35 (○) and 62 nm (▲) hole diameters]. Linear evolution of coercivity H_c with $1/(D-d)$ (D=interhole distance) (Inset).

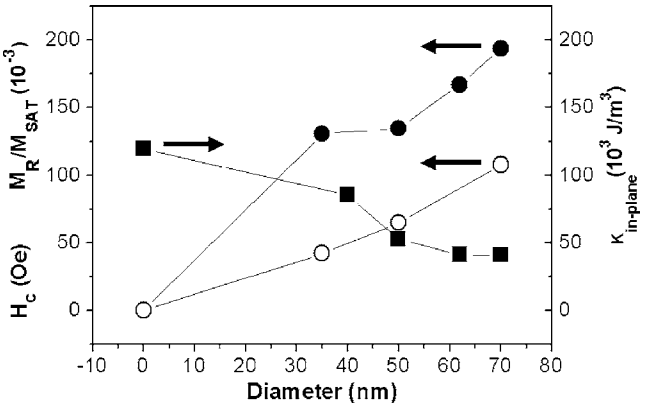

FIG. 5. Coercivity H_c, (●), reduced remanence (M_R/M_{sat}) (○) and in-plane anisotropy (■) as a function of hole diameter.

thus opened to control the coercivity by tailoring the hole diameters and the interhole distances.

Out-of-plane hysteresis loop measurements have been also performed. The loops show a reduced hysteresis and an increase of coercivity, susceptibility, and remanence with nanohole diameter. Figure 5 shows the evolution of coercivity H_c and the ratio remanence to saturation magnetization M_R/M_{sat}, as a function of hole diameter. Estimation of an effective in-plane anisotropy K_{eff} is performed through

$$K_{\text{eff}} = K_{\text{out-of-plane}} - K_{\text{in-plane}} = \int_{0\_\text{out}}^{M_S} \mu_0 H dM - \int_{0\_\text{in}}^{M_S} \mu_0 H dM. \quad (1)$$

Figure 5 also shows the evolution of K_{eff} with hole diameter. The continuous Ni film exhibits a noticeable in-plane anisotropy that is mainly ascribed to the shape anisotropy. Its strength decreases with increasing hole diameter indicating that the hard axis, which is out-of-plane for the continuous Ni film, becomes weaker in the patterned samples.[6] To explain that, we consider that the gaps $(D-d)$ between holes are of 35 and 70 nm, respectively for the samples with the largest (70 nm) and smallest (35 nm) hole diameters, while the thickness of the membrane is 200 nm in all cases. A different "local" shape anisotropy is thus expected, with a stronger contribution to an out-of-plane anisotropy for the case of larger hole diameters. The competition between intrinsic anisotropy and this local shape anisotropy results in the reduction of in-plane anisotropy. In fact, the existence of an out-of-plane anisotropy component has been recently confirmed by Magnetic Force Microscopy imaging.[9]

In summary, Ni nanohole arrays have been fabricated by two-step/positive replication process, using AAM templates with tailored hole diameter. The increase of coercivity in patterned films denotes the pinning effect of the nanoholes. The reduction of the in-plane anisotropy with hole diameter is ascribed to local shape anisotropy effects. Finally, patterning of Ni hole arrays offers possibilities to control magnetic anisotropy and coercivity of these films.

The authors thank U. Gösele who facilitated the work at MPI and J. L. Baldonedo for HRSEM images. The work was supported by the Spanish Ministry of Education and Culture under Project No. MAT04-00150 and Integrated Action Spain-Hungary 2005-7 HH04-0003, and by the German Federal Ministry of Education and Research under project BMBF, FKZ 03N8701.

[1] R. P. Cowburn, A. O. Adeyeye, and J. A. C. Bland, J. Magn. Magn. Mater. **173**, 193 (1997); Appl. Phys. Lett. **70**, 2309 (1997); L. Torres, L. Lopez-Diaz, and J. Iñiguez, *ibid.* **73**, 3766 (1998).
[2] A. O. Adeyeye, J. A. C. Bland, and C. Daboo, Appl. Phys. Lett. **70**, 3164 (1997); U. Welp, V. K. Vlasko-Vlasov, G. W. Crabtree, C. Thompson, V. Metlushko, and B. Llic, *ibid.* **79**, 1315 (2001); I. Ruiz-Feal, L. Lopez-Diaz, A. Hirohata, J. Rothman, C. M. Guertler, J. A. C. Bland, L. M. Garcia, J. M. Torres, J. Bartolome, F. Bartolome, M. Natali, D. Decanini, and Y. Chen, J. Magn. Magn. Mater. **242-245**, 597 (2002); P. Vavassori, G. Gubbiotti, G. Zangari, C. T. Yu, H. Yin, H. Jiang, and G. J. Mankey, J. Appl. Phys. **91**, 7992 (2002).
[3] J. C. Hulteen and C. R. Martin, J. Mater. Chem. **7**, 1075 (1997); J. I. Martin, J. Nogues, K. Liu, J. L. Vicent, and I. K. Schuller, J. Magn. Magn. Mater. **256**, 449 (2003); J. Liang, H. Chik, and J. Xu, IEEE J. Sel. Top. Quantum Electron. **8**, 998 (2002); H. Chik and J. M. Xu, Mater. Sci. Eng., R. **43**, 103 (2004).
[4] Z. L. Xiao, C. Y. Han, U. Welp, H. H. Wang, V. K. Blasco-Vlasov, W. K. Kwok, D. J. Miller, J. M. Hiller, R. E. Cook, G. A. Willing, and G. W. Crabtree, Appl. Phys. Lett. **81**, 2869 (2002); F. J. Castaño, K. Nielsch, C. A. Ross, J. W. A. Robinson, and R. Krishnan, *ibid.* **85**, 2872 (2004).
[5] R. J. Tonucci, B. L. Justus, A. J. Campillo, and C. E. Ford, Science **258**, 783 (1992); D. J. Pearson and R. J. Tonocci, *ibid.* **270**, 68 (1995); M. Park, C. Harrison, P. M. Chaikin, R. A. Register, and D. H. Adamson, Science **276**, 1401 (1997).
[6] H. Masuda and K. Fukuda, Science **268**, 1466 (1995); T. Yanagishita, K. Nishio, and H. Masuda, Adv. Mater. (Weinheim, Ger.) **17**, 2241 (2005); Y. Lei, W-K. Chim, Z. Zhang, T. Zhou, L. Zhang, G. Meng, and F. Phillipp, Chem. Phys. Lett. **380**, 313 (2003).
[7] A. Li, F. Müller, A. Birner, K. Nielsch, and U. Gösele, Adv. Mater. (Weinheim, Ger.) **11**, 483 (1999); K. R. Pirota, D. Navas, M. Hernández-Vélez, K. Nielsch, and M. Vázquez, J. Alloys Compd. **369**, 18 (2004).
[8] H. R. Hilzinger and H. Kronmüller, J. Magn. Magn. Mater. **2**, 11 (1976).
[9] D. Navas, M. Hernández-Velez, A. Asenjo, M. Jaafar, J. L. Baldonedo, and M. Vazquez, IEEE Trans. Magn. **42**, 3057 (2006).